Yazar and Arslan *EURASIP Journal on Wireless Communications and Networking* (2019) 2019:110
https://doi.org/10.1186/s13638-019-1435-z

EURASIP Journal on Wireless Communications and Networking

RESEARCH Open Access

Reliability enhancement in multi-numerology-based 5G new radio using INI-aware scheduling

Ahmet Yazar[1]* and Hüseyin Arslan[1,2]

Abstract

Multi-numerology waveform-based 5G new radio (NR) systems offer great flexibility for different requirements of users and services. However, there is a new type of problem that is defined as inter-numerology interference (INI) between multiple numerologies. This paper proposes novel scheduling and resource allocation techniques to enhance the overall reliability and also provide extra protection for ultra-reliable and low-latency communications (uRLLC) users and cell edge users against INI. Proposed methods are useful for Internet of Things (IoT) communications, and they do not cause additional spectral usage, computational complexity, and latency. Practical INI-aware schemes in this paper include fractional numerology domain (FND) scheduling, power difference-based (PDB) scheduling, and machine learning-based (MLB) scheduling algorithms. INI and signal-to-interference ratio (SIR) results for multi-numerology systems are obtained through computer simulations to show trade-offs between different scenarios and success of the proposed algorithms.

Keywords: 5G, Adaptive scheduling, Machine learning, Multi-numerology, New radio, OFDM, Reliability, Resource allocation, Waveform

1 Introduction

Reliability is one of the key performance metrics of 5th-generation (5G) systems to show the success probability of a transmission. The requirement of 5G reliability is very high compared to long-term evolution (LTE) systems, e.g., ultra-reliable and low-latency communications (uRLLC) service needs 99.999% (five nines) reliability in 5G [1].

There can be various solutions in different communications layers to provide the required reliability. It is also possible to employ different solutions together. Otherwise, it is very difficult to provide the reliability with five nines. Re-transmission schemes are used under media access control (MAC) layer at the expense of additional delays. Physical (PHY) layer solutions like windowing are applied for interference management, but they generally come with an amount of spectral efficiency decrement. Increasing computational complexity, latency, and energy consumption are not preferred for Internet of Things (IoT) communications. In this paper, it is aimed to provide reliability without causing any loss in the other performance metrics including computational complexity, latency, energy consumption, and spectral efficiency. Reliability is enhanced by simple resource allocation and management techniques based on interference-aware scheduling.

One of the most remarkable characteristics of new radio (NR) is its flexibility that is needed for application diversity [2, 3]. Requirements of users (also channel-related issues) and different application groups that include uRLLC, enhanced mobile broadband (eMBB), and massive machine-type communications (mMTC) can only be met with a flexible wireless system [4]. The importance of service multiplexing is increased with the flexibility perpective of multi-numerology-based NR [5, 6]. To support this flexibility, different structures are defined with 5G, and one of them is the multi-numerology waveform design that provides suitable waveform parameters for different types of services at a time. A disadvantage of the

*Correspondence: ayazar@medipol.edu.tr
[1]Department of Electrical and Electronics Engineering, Istanbul Medipol University, 34810 Istanbul, Turkey
Full list of author information is available at the end of the article

multi-numerology systems is the inter-numerology interference (INI) that is a leakage between different numerologies, causing many challenges and presents new research opportunities [7]. Therefore, the importance of adaptive interference management grows. For example, INI is more effective at the edge subcarriers of different numerologies, and signal-to-interference ratio (SIR) of the edge subcarriers is low as a result [7, 8]. It causes unfairness for the edge subcarriers of multiple numerologies, and reliability for the edge subcarriers decreases tremendously. In this paper, INI-aware resource allocation-based scheduling techniques are applied against the multiple numerology-based interference to enhance reliability.

Classical physical resource block (PRB) scheduling algorithms for the resource allocation of single-numerology LTE systems (without INI) are reviewed exhaustively in [9]. Fairness- and reliability-based user equipment (UE) scheduling concept has been extensively studied for single-numerology systems in the literature [10–12]. For example, proportional fair (PF) is one of the most used methods for a fair scheduling [12]. PF scheduling aims to provide fairness while exploiting good channel conditions and dynamically allocating resources to UEs. There are also INI-based reliability enhancement techniques rather than scheduling-based methods in the literature [8, 13]. Most of these techniques (e.g., guard usage, windowing, filtering) do not maintain spectral efficiency and use more spectrum to decrease or eliminate INI effects. However, to the best of the authors' knowledge, INI-aware resource allocation-based scheduling methods without losing from the important performance metrics for reliability enhancement have not been studied intensively under multi-numerology concept. Besides, resource allocation-based scheduling methods can be employed together with the another type of reliability enhancement methods to provide more reliability.

In this paper, fractional numerology domain (FND) scheduling and power difference-based (PDB) scheduling concepts are proposed as main contributions. Moreover, machine learning-based (MLB) scheduling mechanism is provided as another perspective. INI affects all of the users negatively and reliability enhancement can be provided with different solutions to decrease INI effects, but we focus on three ideas under INI-aware resource allocation-based scheduling concepts: (1) protecting uRLLC users from INI more than the other users, (2) protecting cell edge users from INI more than the other users because cell edge users are already subject to interference from the other cells due to their location like in LTE, (3) increasing fairness for the edge subcarriers of multiple numerologies because INI is more effective at the edge subcarriers. The proposed practical solutions aim to enhance the reliability, QoS, and fairness for 5G and beyond communications systems with minimal loss from scheduling flexibility and without bringing additional latency and computational complexity, causing extra energy consumption, and decreasing spectral efficiency. Algorithm designs in this paper can be used also with other reliability enhancement techniques. All of the proposed algorithms are easily implementable with the 3rd Generation Partnership Project (3GPP) standard thanks to the flexible structure of 5G NR.

The rest of the paper is organized as follows: Section 2.1 presents some assumptions on multi-numerology systems in line with the 3GPP standard. FND scheduling concept is introduced in Section 2.2. PDB scheduling algorithms and their backgrounds are described in Section 2.3. An example of MLB scheduling structure is given in Section 2.4. In Section 3, analysis and simulation results for the proposed algorithms are explained. Finally, concluding remarks are provided in Section 4.

2 Methods

2.1 Assumptions and system model

Table 1 shows the 5G numerology parameters including the subcarrier spacing (Δf), CP duration (T_{CP}), and slot duration for data channels in NR according to 3GPP standard documents [7] and [14]. These numerology structures are employed with orthogonal frequency division multiplexing (OFDM), and it is assumed that UEs are synchronous to each other. It is also assumed that the subcarriers (SC) of UEs are non-overlapping to each other and each numerology block that consists of multiple carriers is shared by multiple UEs. We allocate UEs or bandwidth parts (BWP) with the same numerologies contiguously in the frequency domain like in [1, 7, 15].

Algorithms in this paper assume that user-numerology association procedures have been completed in the previous stages of scheduling [2]. For example, base station (BS) assigns NUM-1 to UE-1, 7, 9, 4, and 5 and NUM-2 to UE-6, 8, 3, 10, and 2 in Fig. 1. The proposed INI-aware algorithms may be employed as a feedback of user-numerology association methods, but this paper focuses on the resource allocation of each UEs under the predetermined numerologies.

In [8], a theoretical model for INI is provided for CP-OFDM waveform systems as a special case of windowed OFDM (W-OFDM). INI analysis for a subblock of the numerology with a smaller subcarrier spacing (NUM-1)

Table 1 Numerology structures for data channels in NR

$\Delta f\,(kHz)$	$T_{CP}\,(\mu s)$	Slot duration (ms)	Number of symbols in one slot
15	4.76	1	14
30	2.38	0.5	14
60	1.19 | 4.17	0.25	12 | 14
120	0.60	0.125	14

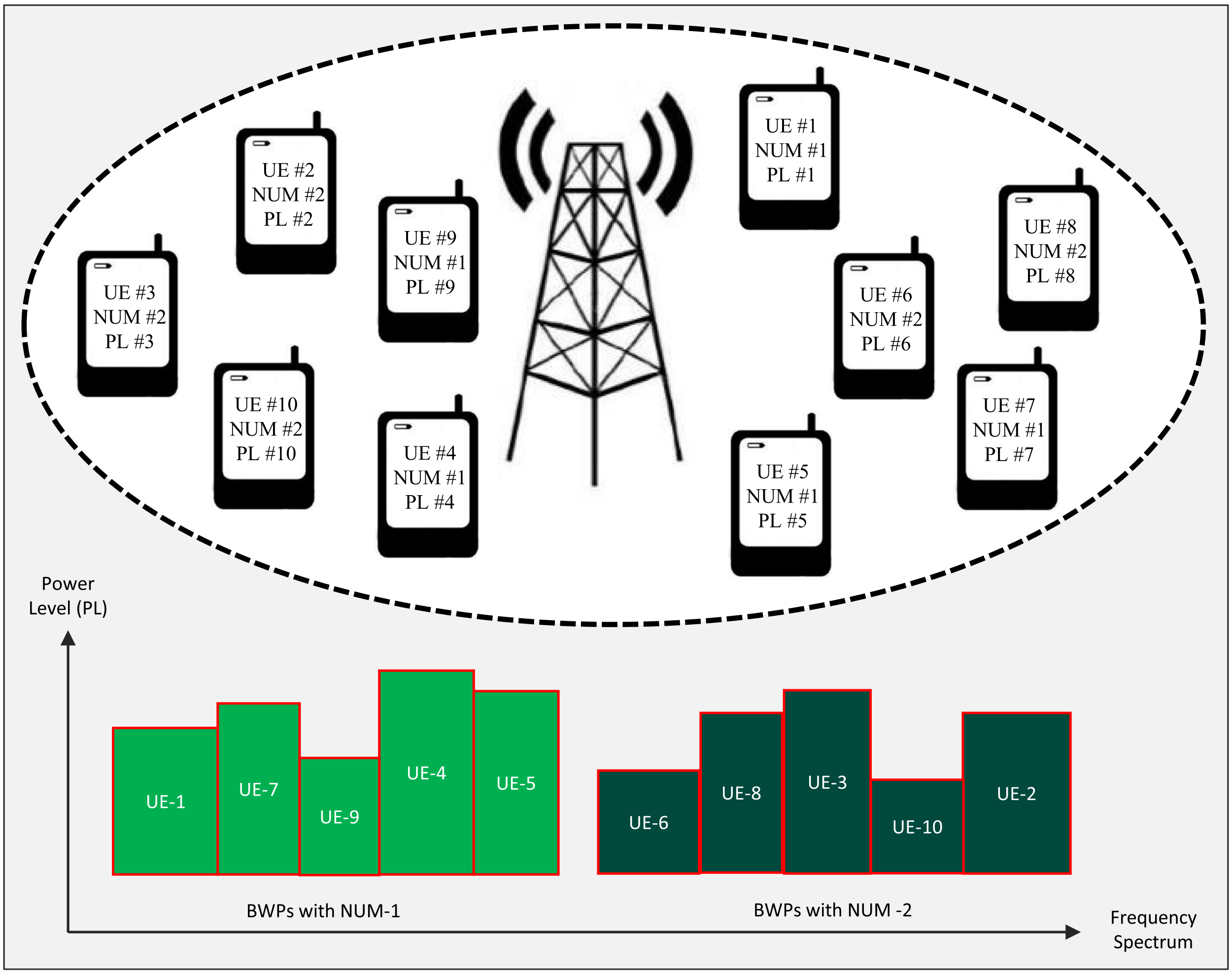

Fig. 1 An example resource allocation in frequency spectrum for the multiple numerologies (NUM) with different user PLs

gives Eq. (1). The result of this equation is the amount of INI that is caused by the other subblock of the numerology with a larger subcarrier spacing (NUM-2). Beside, INI analysis for the subblock of NUM-2 caused by the subblock of NUM-1 gives Eq. (2). These models are taken as a reference in our paper. The detailed derivations of Eqs. 1 and 2 can be found in [8].

$$P_u{}^{(1)}(k) \approx \frac{|\rho^{(2)}H^{(2)}(u)|^2}{N^{(2)}N^{(1)}}\left[\left|\frac{\sin\left[\frac{\pi}{N^{(1)}}\Delta k^{(1)}\alpha N_T{}^{(2)}\right]}{\sin[\frac{\pi}{N^{(1)}}\Delta k^{(1)}]}\right|^2 + (\alpha-1)\left|\frac{\sin\left[\frac{\pi}{N^{(1)}}\Delta k^{(1)}N_T{}^{(2)}\right]}{\sin[\frac{\pi}{N^{(1)}}\Delta k^{(1)}]}\right|^2\right] \quad (1)$$

$$P_u{}^{(2)}(k) \approx \frac{|\rho^{(1)}H^{(1)}(u)|^2}{N^{(2)}N^{(1)}}\left|\frac{sin\left[\frac{\pi}{N^{(1)}}\Delta k^{(2)}N^{(2)}\right]}{sin[\frac{\pi}{N^{(1)}}\Delta k^{(2)}]}\right|^2 \quad (2)$$

Here, $P_u{}^{(i)}(k)$ is the INI power on the kth subcarrier of NUM-i that is caused by the uth subcarrier of the other subblock. $\rho^{(i)}$ is the power adjusting factor for the subblock with NUM-i. $H^{(i)}(u)$ is the channel frequency response on the uth subcarrier of the subblock with NUM-i. $N^{(i)}$ is the discrete fourier transform (DFT) length, and $N_T{}^{(i)}$ is the symbol duration (regarding the number of samples) for OFDM symbols. $\Delta k^{(i)}$ is the spectral distance between the subcarrier k of the subblock with NUM-i and the interfering subcarrier of the other subblock. α is the number of rectangular overlapping windows.

Increasing spectral distance between subcarriers with different numerologies decreases INI effects. Then, using a guard band between different numerologies is one way to decrease INI in return to spectral efficiency. The 3GPP standards make guard band choices flexible with high granularity [7]. Various amounts of guard bands are used while comparing the results in the next sections. Moreover, it is assumed that each UE has different power levels (PLs) as shown in Fig. 1, and this variation is exploited in the proposed PDB scheduling algorithms.

FND is a novel resource allocation structure. In the proposed structure, there are inner and outer users for each subblocks with different numerologies as shown in Fig. 2. All of the outer users are also candidate edge users. Additionally, outer users are divided into non-edge outer users and edge users. INI effects decrease from edge users to inner users. Fractional regions of each subblocks are used while applying scheduling algorithms. These regions are not fixed parts of the numerology subblocks.

It is assumed that UEs have independent and identically distributed multipath Rayleigh fading channels, and perfect channel state information (CSI) is obtained at the receiver sides. Additionally, re-use factor is one in all cells like in LTE systems. Hence, inter-cell interference is more effective in the cell edges.

2.2 Fractional numerology domain scheduling

Users can be scheduled using the FND concept to protect some of the users from INI effects more. Inner parts of the numerology subblocks are not affected by INI in comparison with outer parts of the subblocks. Therefore, extra protection against the INI effects can be provided by locating some of the users who need more reliability into the inner parts of the numerology subblocks. In the next sections, two ideas are presented to ensure that uRLLC users and cell edge users are protected from INI effects more as also shown in Fig. 3.

INI analysis results regarding Eqs. 1 and 2 for multiple numerologies with different subcarrier spacings and guard bands are presented in Fig. 4. Guard band (GB) usage increases spectral distance between the numerologies, and it decreases INI. However, the amount of INI is calculated more at the numerology edges in all scenarios. Total INI and INI variation between inner and outer users decrease with the usage of GB in return to corresponding spectral efficiency. Additionally, if subcarrier spacing difference between the numerologies increase, it affects INI negatively.

Equation 3 is derived to calculate the total regional INI effects on different subcarriers of a subblock. It is obtained for the total amount of regional INI caused by the other subblock with a different numerology. Here, a and b define a region in one subblock. This region can be only one subcarrier or whole subblock. $P^{(i)}(a,b)$ gives the total interference power at the target region of a subblock with NUM-i. $Z^{(j)}$ presents the number of contiguous subcarriers in the other subblock with NUM-j, and it is assumed that $0 \leq a \leq b < Z^{(j)}$.

$$P^{(i)}(a,b) = \sum_{k=a}^{b} \sum_{u=0}^{Z^{(j)}-1} {P_u}^{(i)}(k) \tag{3}$$

Inner users are affected less than edge users for one numerology. Table 2 provides total regional INI powers regarding Eq. (3) for different users while GB is varying. As it can be seen from Table 2, GB usage has more effects at the edges compared to the inner parts of numerologies. Reliability of numerology edges always less than the other parts of numerologies in frequency domain. For the five nines reliability, numerology edges are not safe enough even there is a a reasonable GB between multiple numerologies.

2.2.1 Reliability enhancement for uRLLC users

uRLLC users can be assigned to subblocks with different numerologies. There is not a specific 5G numerology that fits best with uRLLC service. Some of the 5G numerologies include large Δf that is better to struggle with inter-carrier interference (ICI) problems and also better regarding low-latency requirements. However, T_{CP} changes directly proportional with symbol duration $(1/\Delta f)$ in 5G. It may cause inter-symbol interference (ISI)

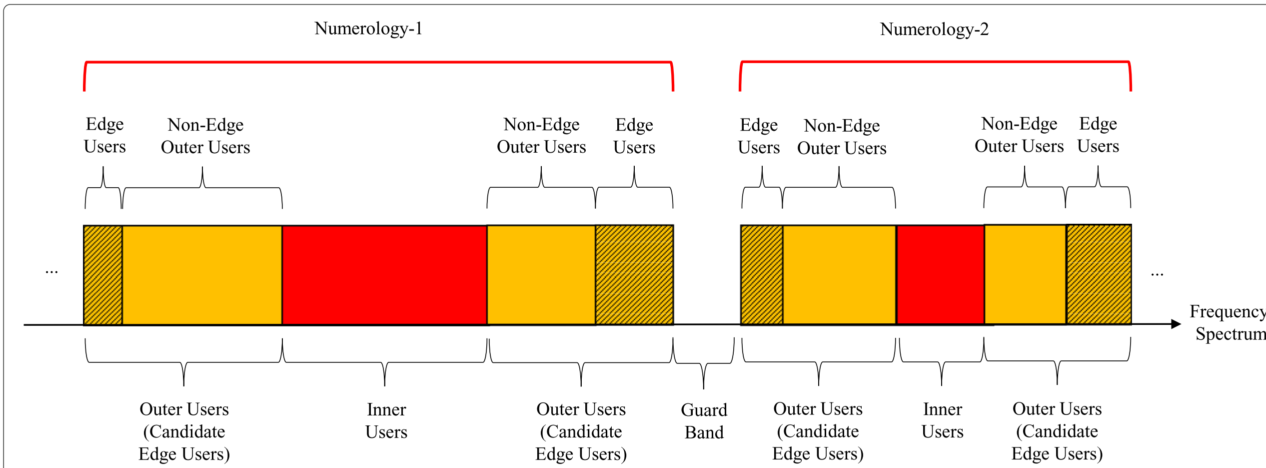

Fig. 2 Fractional numerology domain (FND) structure

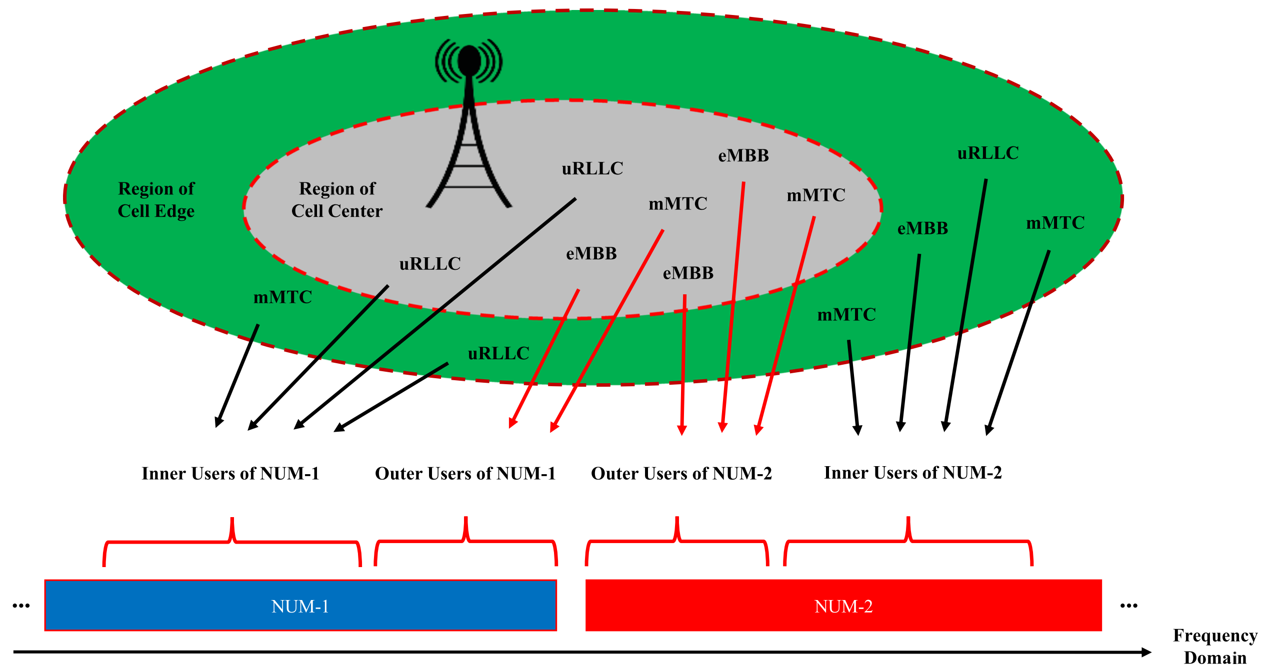

Fig. 3 Protection for uRLLC users and region of cell edge users. It is assumed that there are inter-cell interference in the region of cell edges. Inner regions of the subblocks are safer than the outer regions

problems because large Δf (short symbol duration and short T_{CP}) is not suitable for long delay spread cases. ISI problems decrease reliability.

We are proposing that uRLLC data should be scheduled at more reliable regions of multiple numerologies considering its importance. We need to protect uRLLC users more compared to the other users. Hence, uRLLC users can be assigned as inner users of suitable numerologies. If all users are associated with uRLLC service exceptionally (e.g., vehicle-to-vehicle communications in highways), all subcarriers (inner and outer) of a subblock can be employed for uRLLC service.

2.2.2 Reliability enhancement for cell edge users

Re-use is taken as one in LTE and beyond systems. Therefore, all of the channels can be employed in all cells. It causes an extra interference on the cell edge users. If there is a fractional cell with two clusters as a region of cell edge and region of cell center like in Fig. 3, users in the region of cell edge are exposed to inter-cell interference more compared to users in the region of cell center. Reliability is provided better in the region of cell center inherently thanks to path loss effects of the wireless channel.

In the proposed idea, we do not want to schedule the same user at the cell edges and the numerology edges. Two disadvantages together are too much unfairness for a user. Cell edge users at least need to be protected from INI effects more. Hence, cell edge users are scheduled as inner users of the subblocks with suitable numerologies.

2.2.3 User priorities for INI protection

It is also possible to enhance the reliability for uRLLC users and cell edge users together. For this purpose, uRLLC users and cell edge users can be scheduled to the inner parts of the subblocks as far as possible. Three types of special users are listed as (1) association with the uRLLC service, (2) being at the cell edge, and (3) being at the numerology edge. If two of them are valid for one user, it is a bad luck. Moreover, if all of these situations are valid for one user, it is the worst case scenario. We cannot control the first two cases, but being at the numerology edge can be controlled by the scheduler. At that point, the inner users of the subblocks can be decided by starting with the worst case scenario. Some priorities are defined for our algorithms as shown in Fig. 5. They can be listed as (1) association with the uRLLC service and being at the cell edge, (2) association with the uRLLC service and being at the cell center, (3) association with the non-uRLLC service and being at the cell edge, and (4) association with the non-uRLLC service and being at the cell center. After the inner users of subblocks are decided, scheduling of these users on the frequency domain is employed flexibly because the proposed design aims to maintain scheduling flexibility as much as possible. Scheduling each user on specific subcarriers decreases
flexibility.

For the non-inner or outer users of subblocks, our scheduling algorithms are described in the next section.

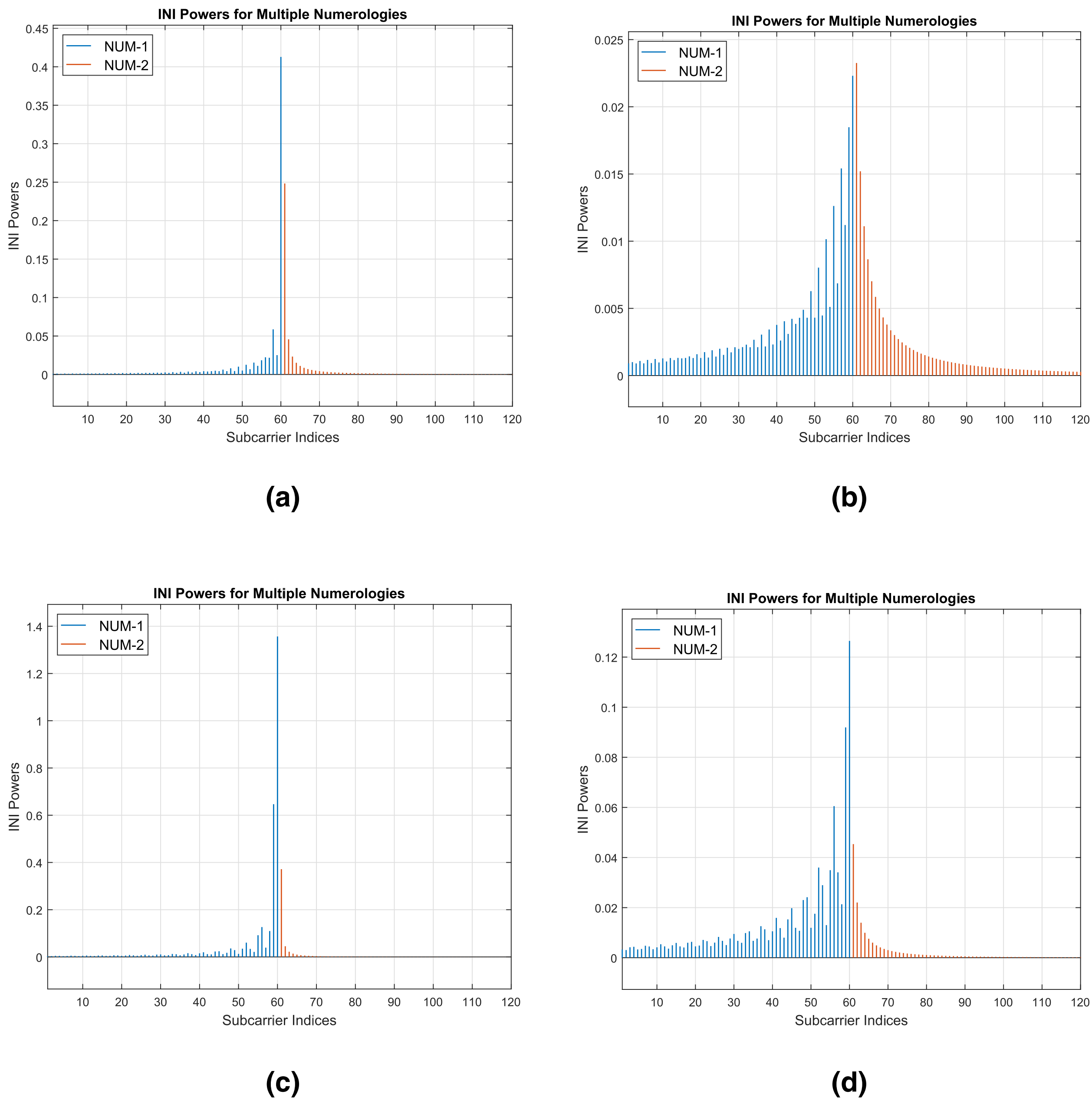

Fig. 4 INI analysis results regarding Eqs. 1 and 2 for multiple numerologies with different subcarrier spacings and guard bands. **a** NUM-1 has narrow SCs with 15 kHz, and NUM- 2 has wide SCs with 30 kHz. There is not any GBs between the numerologies. **b** NUM-1 has narrow SCs with 15 kHz, and NUM-2 has wide SCs with 30 kHz. There are four SCs as GBs between the numerologies. **c** NUM-1 has narrow SCs with 15 kHz, and NUM- 2 has wide SCs with 60 kHz. There is not any GBs between the numerologies **d** NUM-1 has narrow SCs with 15 kHz, and NUM-2 has wide SCs with 60 kHz. There are four SCs as GBs between the numerologies

2.3 Power difference-based scheduling

Outer users (candidate edge users) are investigated to find the best suitable edge users of subblocks in this section. Power level (PL) and bandwidth (BW) of a UE are considered as the two main inputs for the proposed PDB scheduling methods. Fairness of UEs at the numerology edges is increased by minimizing the INI effects while maintaining spectral efficiency with fixed guard bands. The overall reliability is also enhanced by our novel scheduling methods. We focus only on candidate edge UEs in the proposed algorithms. After the decision of edge users, the other outer UEs can be scheduled flexibly in the

Table 2 Total INI powers on each user or subblock regarding Eq. (3) for different guard bands between two numerologies

	NUM-1					NUM-2				
	Inner part		Outer part			Outer part			Inner part	
	UE-1	UE-2	UE-3	UE-4	UE-5	UE-6	UE-7	UE-8	UE-9	UE-10
INI power (GB: 0 SCs)	0.0139	0.0193	0.0301	0.0544	0.6205	0.3816	0.0233	0.0107	0.0062	0.0041
INI power (GB: 6 SCs)	0.0122	0.0161	0.0239	0.0390	0.0937	0.0725	0.0185	0.0092	0.056	0.0038
INI power (GB: 12 SCs)	0.0108	0.0139	0.0193	0.0301	0.0544	0.0438	0.0150	0.0080	0.0050	0.0035
INI power (GB: 24 SCs)	0.0084	0.0108	0.0139	0.0193	0.0301	0.0233	0.0107	0.0062	0.0041	0.0028
INI power (GB: 36 SCs)	0.0069	0.0084	0.0108	0.0139	0.0193	0.0150	0.0080	0.0050	0.0035	0.0025

NUM-1 has narrow SCs with 15 kHz, and NUM-2 has wide SCs with 30 kHz. UE-5 and UE-6 are located at numerology edges in frequency domain. UEs have equal number of SCs

frequency domain. Hence, scheduling flexibility does not lose.

In the next sections, power difference problem for the edge users of numerologies is analyzed. Then, novel algorithms are proposed to increase fairness and reliability by scheduling users at the edges of multiple numerologies more carefully.

2.3.1 Power difference for the edge users of different numerologies

INI is generally concentrated at the edge SCs of subblocks because of the large side lobes and non-orthogonality of multiple numerologies [7, 16]. In addition to the INI problem for the UEs on numerology edges, power difference is another issue for multi-numerology systems [17]. SIR degradation occurs especially at the edge UEs in different numerologies. Power offset (PO) affects SIR negatively. Combined effects of INI and power difference on SIR are given by Eq. (4). In these equation, $\mathrm{SIR}_u{}^{(i)}(k)$ is SIR on the kth subcarrier of NUM-i that is caused by the uth subcarrier of the other subblock. $PL^{(i)}(k)$ is power level on the kth subcarrier of NUM-i and $\mathrm{PL}^{(i)}(u)$ is the power level on the uth subcarrier of NUM-i. If i is 1, j is taken as 2, and if i is 2, j is taken as 1.

$$\mathrm{SIR}_u{}^{(i)}(k) = \frac{\left[\mathrm{PL}^{(i)}(k)\right]^2}{\left[\mathrm{PL}^{(j)}(u)\right]^2 P_u{}^{(i)}(k)} \tag{4}$$

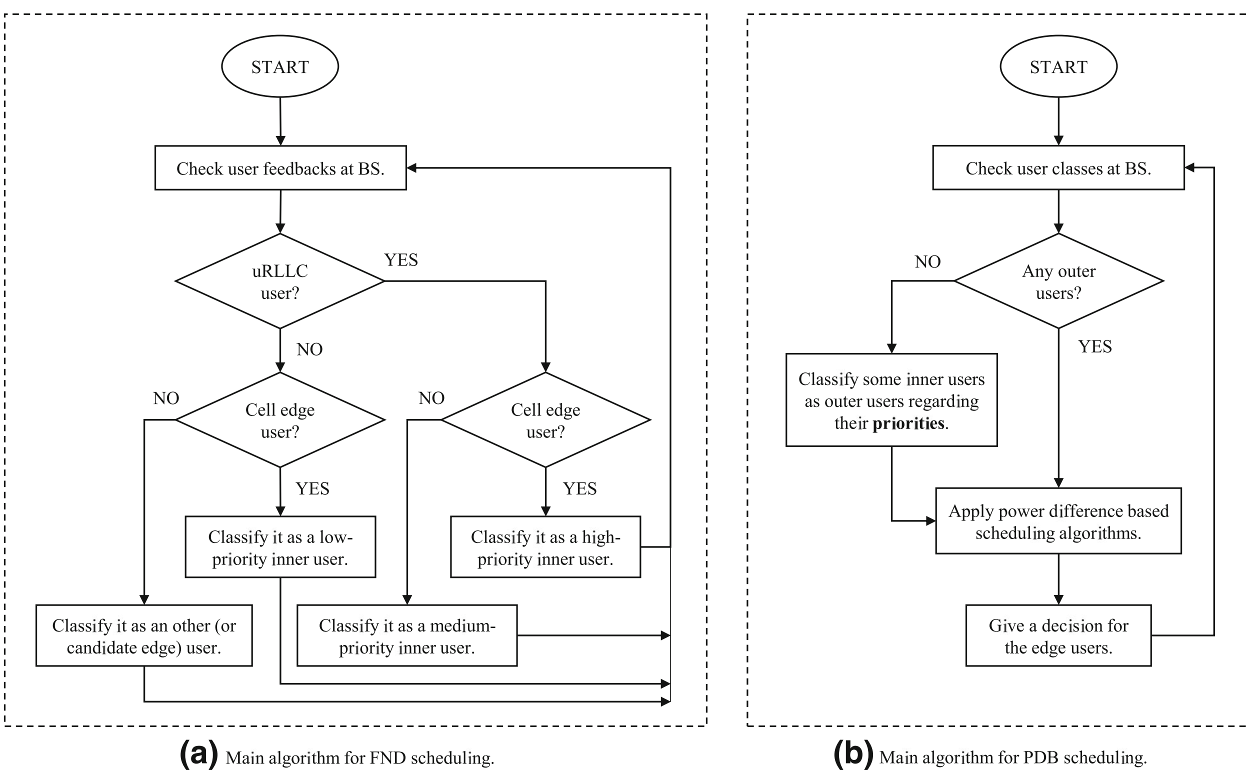

Fig. 5 Flowcharts of the proposed main algorithms for **a** FND scheduling and **b** PDB scheduling

Power difference between UEs of different numerologies increases the effects on SIR. Hence, fairness and reliability for the edge UEs of numerologies need to be provided under different PLs while maintaining the other performance criteria. PO for the edge UEs can be minimized to increase the fairness for the edge UEs. Also, minimizing a variance between SIR values for different cases aims the same motivation. SIR values of one UE should not change noticeably with time. Weak UEs are affected easily by high POs like in the near-far problem for a cell. It causes higher SIR variances and low reliability for these UEs. There is a need to balance SIR to preserve the reliability of UEs and protect weak UEs.

A lower PO can also be useful to minimize guard necessities between different numerologies under desired SIR [17]. In that case, spectral efficiency can be increased due to the fewer guards. Authors of [17] aim to minimize guard necessities with a fixed SIR and fairness in their scheduling algorithm. However, we increase the fairness and SIR for the weak UEs to protect them under fixed guards and spectral efficiency. Reliability requirement has a higher priority in our scenario.

In this paper, it is assumed that there are multiple users with different PLs in the same numerology. However, all users have different numerology parameters in [17]. They put each user in a specific place regarding their PLs. It causes a low scheduling flexibility. We propose PDB scheduling algorithms that focus only edge users of the subblocks to maximize fairness and reliability for UEs of contiguous multiple numerologies.

There are two goal functions. The first of them is about the interaction between edge UEs of the numerologies, and it is more important because most of the INI is concentrated on the numerology edges. We need to maximize SIR at the edge users. The second goal function is focused on the interaction between one edge UE of one numerology and the inner UEs of the other numerology. In this case, we can also enhance SIR on the inner UEs.

The proposed fairness-aware scheduling algorithms are presented in Fig. 6. The first part shows a random scheduling case, and the other parts show the proposed scheduling mechanisms. Algorithm 1 maximizes the fairness and reliability of edge UEs. Algorithm 2 checks the non-edge outer UEs in addition to edge UEs if the narrow BW UEs are scheduled at the numerology edges as a decision of algorithm 1. There are small trade-offs between the proposed algorithms as shown in Table 3.

2.3.2 Algorithm 1: Scheduling based on edge user reliability

This method schedules UEs as a function of POs between the UEs for different numerologies. In Fig. 6b, the frequency positions of UE-6 and UE-7 are replaced with each other in the same numerology. UE-4 and UE-5 are also switched at the NUM-1 side. Hence, the PO between edge UEs (UE-4 and UE-7) is minimized to ensure that SIR is maximized at the subblock edges. Equation 4 shows that PO directly effects SIR values with the INI problem. Additionally, Eqs. 1 and 2 prove that spectral distance between the subcarriers of different numerologies is very important in INI analysis and numerology edges are the closest regions to each other. Hence, most of the INI are exposed by numerology edges.

There can be more than two numerologies at a time, but our algorithm works based on numerology pairs like in Fig. 6. The algorithm needs to be employed for each of the contiguous two numerologies. For this reason, it is assumed that there are two numerologies in the remaining parts of the paper.

There are E non-URLLC users ($u_{1,1}$, $u_{1,2}$, ... ,$u_{1,E}$) for NUM-1, and F non-URLLC users ($u_{2,1}$, $u_{2,2}$, ... ,$u_{2,F}$) for NUM-2. PLs of these users are $\left(\mathrm{PL_1}^{(1)}, \mathrm{PL_2}^{(1)}, ..., \mathrm{PL}_E{}^{(1)}\right)$ and $\left(\mathrm{PL_1}^{(2)}, \mathrm{PL_2}^{(2)}, ..., \mathrm{PL}_F{}^{(2)}\right)$, respectively. Then, there are totally $E \times F$ possibilities for the PO values between UE pairs with different numerologies. The smallest power difference selection is made using Eqs. 5 and 6. Then, the resulting UE pair, $(s,t)^*$, can be located at the edges of numerologies to increase reliability for edge UEs.

$$\mathrm{PO}(s,t) = |\mathrm{PL}_s{}^{(1)} - \mathrm{PL}_t{}^{(2)}| \tag{5}$$

$$(s,t)^* = \underset{(s,t)}{\operatorname{argmin}}\, \mathrm{PO}(s,t) \tag{6}$$

where s and t are UEs for NUM-1 and NUM-2, respectively. $\mathrm{PO}(s,t)$ is the related power offset value.

2.3.3 Algorithm 2: Scheduling based on edge user reliability with considering the BWs of UEs

If the edge UEs are scheduled without considering the BWs of UEs, narrow BW users can be located at the edges of numerologies. In this case, important parts of one numerology's INI effects can continue through more UEs after the narrow BW edge UE. It causes to focus on more than one UE at the side of narrow BW edge UE. For example, frequency positions of UE-6 and UE-10 are replaced with each other after applying algorithm 1 as shown in Fig. 6c. Hence, the POs between UE-4 and UE-10 are minimized to ensure that SIR is maximized through UE-10 that is located next to the narrow BW edge UE.

Algorithm 2 can be applied after algorithm 1 if there is a narrow BW edge UE. The decision to employ algorithm 2 is given by checking SIR at the outermost subcarrier of a UE next to the edge UE. Total SIR value at a specific subcarrier, a, can be calculated using Eq. (7). Here, $Z^{(j)}$ presents the number of contiguous subcarriers in the other subblock with NUM-j, and it is assumed that $0 \leq u < Z^{(j)}$.

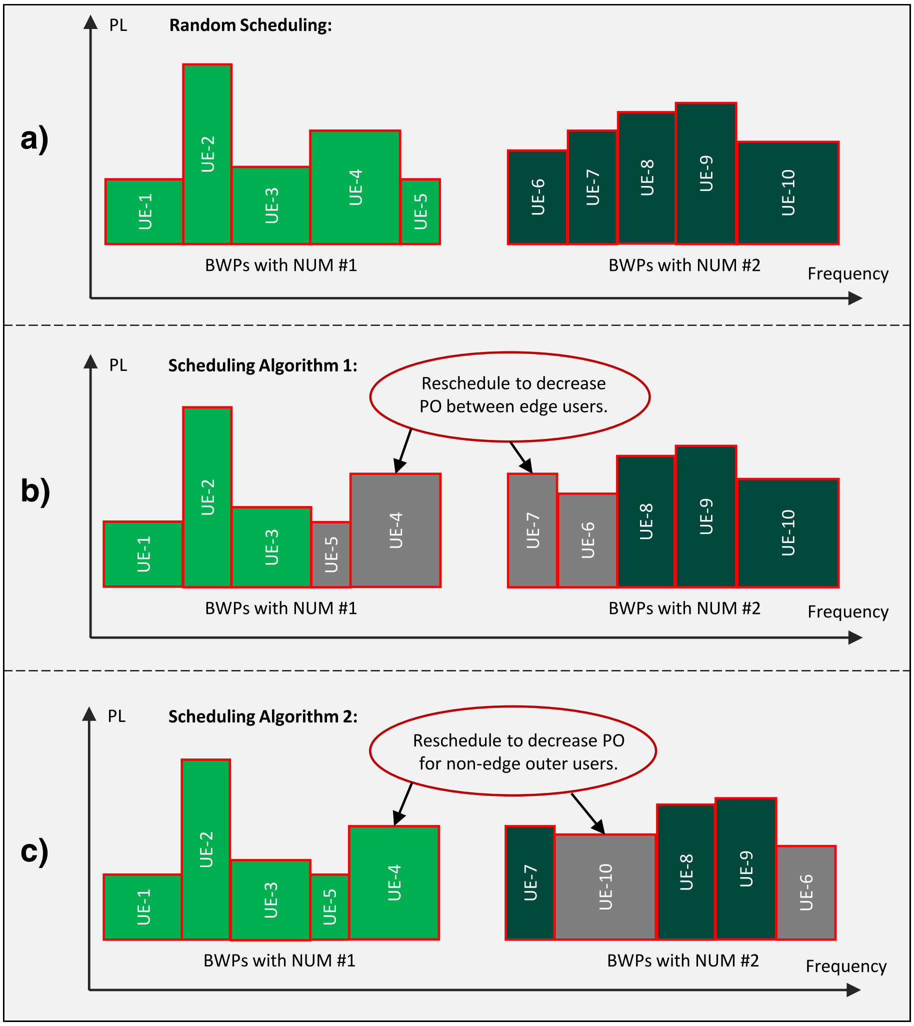

Fig. 6 Representation of proposed PDB scheduling algorithms to decide on edge users for multi-numerology systems. There is a fixed guard band between two different numerologies. It is assumed that PO between UE-4 and UE-7 is less than the PO between UE-4 and UE-10. Moreover, PO between UE-4 and UE-10 is less than the PO between UE-3 and UE-6. **a**) Random Scheduling. **b**) Scheduling Algorithm-1. **c**) Scheduling Algorithm-2

$$\mathrm{SIR}^{(i)}(a) = \frac{\left[\mathrm{PL}^{(i)}(a)\right]^2}{\sum_{u=0}^{Z^{(j)}-1}\left[\mathrm{PL}^{(j)}(u)\right]^2 {P_u}^{(i)}(a)} \tag{7}$$

Equation 7 gives total SIR at a subcarrier by all other subcarriers while Eq. (4) is calculating SIR at a subcarrier by only one other subcarrier. $\mathrm{TH}_{\mathrm{SIR}}$ is a threshold value for desired total SIR at one subcarrier and if $\mathrm{SIR}^{(i)}(a) < \mathrm{TH}_{\mathrm{SIR}}$ at the subcarrier of a, it means algorithm 2 needs to be employed after algorithm 1 to find the most suitable UE, r^*, that can be located next to the edge UE.

Table 3 Basic comparison of the algorithms

	Advantages	Disadvantages
Random scheduling	The best scheduling flexibility	Cannot provide fairness especially for edge UEs
Algorithm 1	Maximizes SIR at the edge UEs; good scheduling flexibility.	No enhancement for non-edge outer users' SIR
Algorithm 2	Maximizes SIR at the edge UEs; additionally protects non-edge outer users more than algorithm 1; increases overall SIR	A small loss in scheduling flexibility
Proportional fair	Increases SIR at the edge UEs compared to random scheduling	Cannot provide the best SIR for edge UEs while balancing fairness between all UEs

Equation 8 is used to find r^* by comparing the power differences between edge UE of the other subblock and all UEs except edge UE in the current subblock. In other words, algorithm 1 is repeated to find a single user rather than a user pair. If r^* is searched for NUM-1, there are $F-1$ possibilities for the PO values. Otherwise, the number of possibilities for the PO values is $E-1$. Edge UEs that are found in algorithm 1 are not candidates for r^* in Algorithm 2.

$$r^* = \underset{r}{\operatorname{argmin}}\, A \tag{8}$$

where A is PO based on Eq. (5) and can be calculated using Eq. (9). Here, s_{edge} and t_{edge} are edge UEs that are found with algorithm 1. The number of r^* can be 1 or 2. If there is only one narrow BW edge UE, the number of r^* is 1. If there are narrow BW UEs at both numerology edges, the number of r^* is 2.

$$A = \begin{cases} PO(r, t_{\text{edge}}), & \text{if } r \text{ is using NUM-1} \\ PO(s_{\text{edge}}, r), & \text{if } r \text{ is using NUM-2} \end{cases} \tag{9}$$

Algorithm 2 causes a small decrement in scheduling flexibility, but it protects non-edge outer UEs more than algorithm 1 and increases overall SIR. If there are large BW users at the numerology edges, algorithm 1 is enough and we do not need to employ algorithm 2. Equations 1, 2, and 4 provide an optimization objective for algorithm 1 while the same equations and Eq. (7) form an optimality background for algorithm 2. Computational complexity of the proposed algorithms are low since they are practical methods. Alternatively, these algorithms can also be implemented using ML type of decision mechanisms. An example ML concept is presented in the next section.

2.4 Machine learning-based scheduling

ML is used for different wireless communications problems in the last years [18–20]. ML-based (MLB) solutions can provide promising results for different applications of wireless communications. Figure 7 shows an example-supervised learning illustration for a MLB scheduling decision mechanism that can be used instead of the proposed algorithms in this paper.

There is a need for a large dataset to train ML systems. Otherwise, ML cannot get high performances compared to the non-ML techniques. Large datasets can be formed as measurement or simulation-based methods. Measurement-based dataset generation requires too many different measurements under all scenarios. Hence, simulation-based dataset generation is more preferable than the measurement-based methods. For example, class labels of each input vector for one million random cases need to be decided in a simulation. Maximization on the SIR values of UEs can be used as a decision unit while forming the dataset for each of one million scenarios. The simulation-based dataset can be formed considering FND and PDB scheduling objectives together.

After forming the dataset with input vectors and corresponding class labels, supervised training process can be employed for different ML or fuzzy logic methods. Then, the trained models are used as a solution to provide reliability enhancement in our resource allocation-based scheduling problem. At this point, dataset generation and training ML models with this dataset are left as a future work.

3 Results and discussion

In the performance analysis simulations, it is assumed that there are 5 UEs in each numerology like in Fig. 6 for the sake of clarity. However, there are 42 UEs in each numerology for simulation results of 3 algorithms. Some other simulation parameters are provided in Table 4.

Δf_{ref} kHz and $2^k \times \Delta f_{\text{ref}}$ kHz SC spacings are used for two numerologies, where 2^k is the scaling factor and k is a positive integer. N_{ref}-point and $N_{\text{ref}}/(2^k)$-point inverse fast Fourier transform (IFFT) blocks are employed by NUM-1 and NUM-2, respectively. After each IFFT operation, CP samples are added with a ratio of CP_{R} to every OFDM symbol in each numerology. It is assumed that UEs have independent and identically distributed multipath Rayleigh fading channels, and perfect channel state information (CSI) is obtained in the receiver. At the receiver side, N_{ref}-point and $N_{\text{ref}}/(2^k)$-point fast Fourier transform (FFT) blocks are used by NUM-1 and NUM-2, respectively. The same structure is used for the rest of this section.

3.1 Performance analysis of fractional numerology domain scheduling for different power levels

Theoretical analysis results in Section 2.2 show that the inner parts of subblocks with different numerologies are on the safe side regarding the INI effects. Besides, most of the INI is gathered in the edge subcarriers and users of each subblocks. All of the UEs have equal PLs and the same number of SCs in Section 2.2.

Here, POs of the UEs alternate between 0 and 7 dB. INI and SIR estimations are done for each of the used SCs separately. Monte Carlo method is applied to increase the statistics in the performance results. The number of independent tests is 1000, and different set of random data is used in each of these tests. Thereafter, the average INI and SIR on the SCs are estimated. Estimations are done with a simulation-based script and analytical equation-based script separately under the same conditions. Simulation-based SIR results are presented and

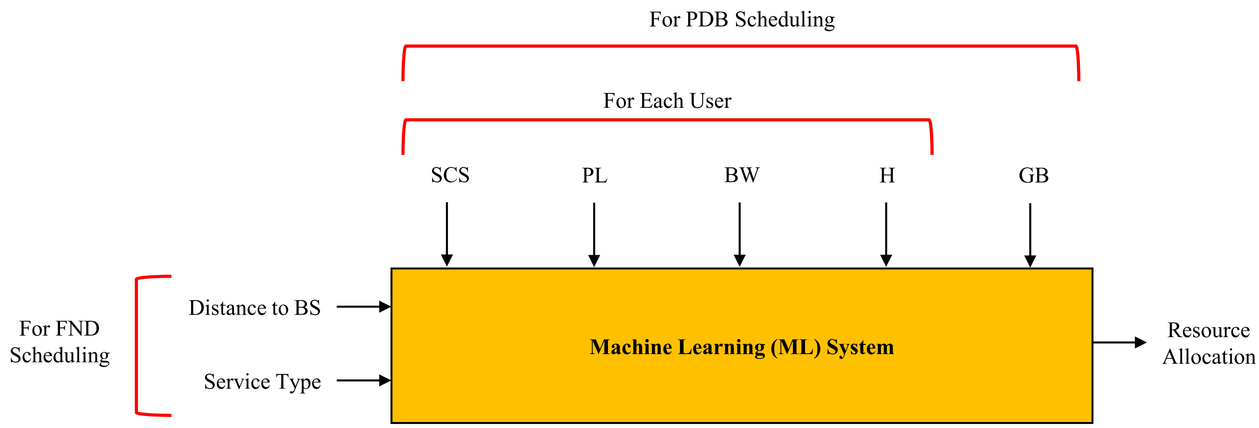

Fig. 7 An example ML block diagram. Distance to BS and service type are inputs for FND scheduling. Subcarrier spacing (SCS), PL, BW, and wireless channel (*H*) are used as inputs of PDB scheduling for each UE. Guard band (GB) between two numerologies is used as another input for PDB scheduling

compared with analytical SIR results in Fig. 8 with the below inferences:

1 If case 1 and case 3 are compared to each other, it can be seen that the SIR results at the edge UE of NUM-1 decrease about 14 dB while SIR values at all UEs of NUM-2 increase between 9 and 11 dB in case 3. Scheduling edge UEs with different PLs causes this unfairness. Reliability for edge UE is very low in case 3 because of the PO.
2 If case 3 and case 5 are compared to each other, high PL UE is shifted from the edge to the inner side in case 5. Then, there is not any PO between the edge UEs. There are SIR increments of 6–14 dB at the edge UE and 1.5–6 dB at the non-edge UEs of NUM-1. SIR results of all UEs of NUM-2 stay above 14 dB in case 5.
3 If there is a GB of six SCs between the numerologies (case 2, case 4, and case 6), SIR values for the edge UEs increase between 1 (non-edge side) and 17 dB (edge side). GB usage enhances the SIR in exchange for some spectrum resources, but it does not change the truth that numerology edges always have more INI.

All of these results and inferences show that the inner parts of the numerology subblocks are better against INI effects. Then, they also show that FND scheduling is a meaningful mechanism to provide an extra protection for some of the users. On the other side, PDB scheduling algorithms are also useful for different cases. As an example, the proposed algorithms try to make a resource allocation-based scheduling similar to case 1 and case 5.

Table 4 Simulation parameters for multiple numerologies

The number of users for NUM #1	E	5 or 42
The number of users for NUM #2	F	5 or 42
Reference value for Δf	Δf_{ref}	15 kHz
The scaling factor for Δf	k	1
Reference size of IFFT/FFT blocks	N_{ref}	4096
CP ratio	CP_{R}	1/16

3.2 Simulation results for power difference-based scheduling

In this section, PL offsets are generated 200 times randomly between 0 and 10 dB. Usable SCs for each UEs change randomly in each independent test. Proposed scheduling algorithms are compared with the random scheduling and PF scheduling cases. GB usage scenarios are also included with the algorithm results. The main aim of our scheduling algorithms is to minimize the variance between SIR values for different cases. SIR values of one user should not change noticeably with time to provide a high reliability. There is too much fluctuation in SIR at the edge UEs of different numerologies for the random scheduling scenario. Proposed algorithms balance SIR to preserve the fairness between users. The amount of INI is took into account with channel conditions for the PF scheduling to balance fairness regarding INI. Cumulative distribution function (CDF) curves are used to show the statistical results of all methods.

CDF curves for the edge UEs are presented in Fig. 9a, b for without GB and with GB cases. Here, the number of usable SCs are taken randomly for all users. CDF curves show that the variance in SIR for our all algorithms are lower than the random scheduling case for the edge UEs. Therefore, fairness and reliability of the edge UEs are enhanced by using fairness- and reliability-aware scheduling methods. Algorithm 1 and algorithm 2 give better results than the random scheduling and PF

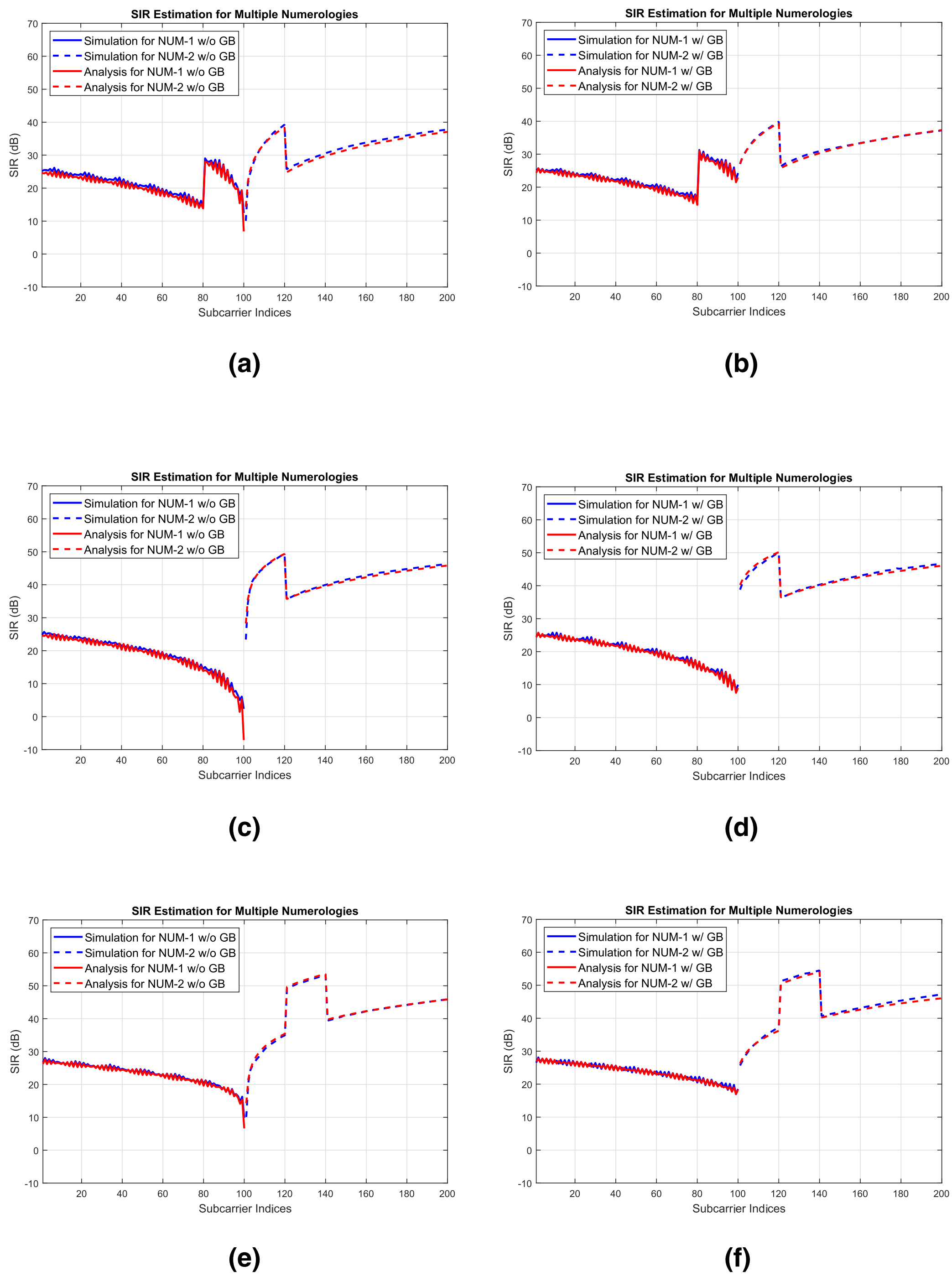

Fig. 8 Performance analysis results for different cases. NUM-1 has a narrow SCs with 15 kHz Δf, and NUM-2 has a wide SCs with 30 kHz Δf. If there is a PO, it is 7 dB. There are five UEs for NUM-1 and five UEs for NUM-2 with equal number of SCs. **a** Case 1: edge UEs of NUM-1 and NUM-2 have higher PLs than the other UEs. There is not any POs between the edge UEs. There is not any GB between numerologies. **b** Case 2: edge UEs of NUM-1 and NUM-2 have higher PLs than the other UEs. There is not any POs between the edge UEs. There is a GB of six SCs between numerologies. **c** Case 3: edge UE of NUM-2 has a higher PL than the other UEs. There is not any GB between numerologies. **d** Case 4: edge UE of NUM-2 has a higher PL than the other UEs. There is a GB of six SCs between numerologies. **e** Case 5: non-edge UE of NUM-2 has a higher PL than the other UEs. There is not any GB between numerologies. **f** Case 6: non-edge UE of NUM-2 has a higher PL than the other UEs. There is a GB of six SCs between numerologies

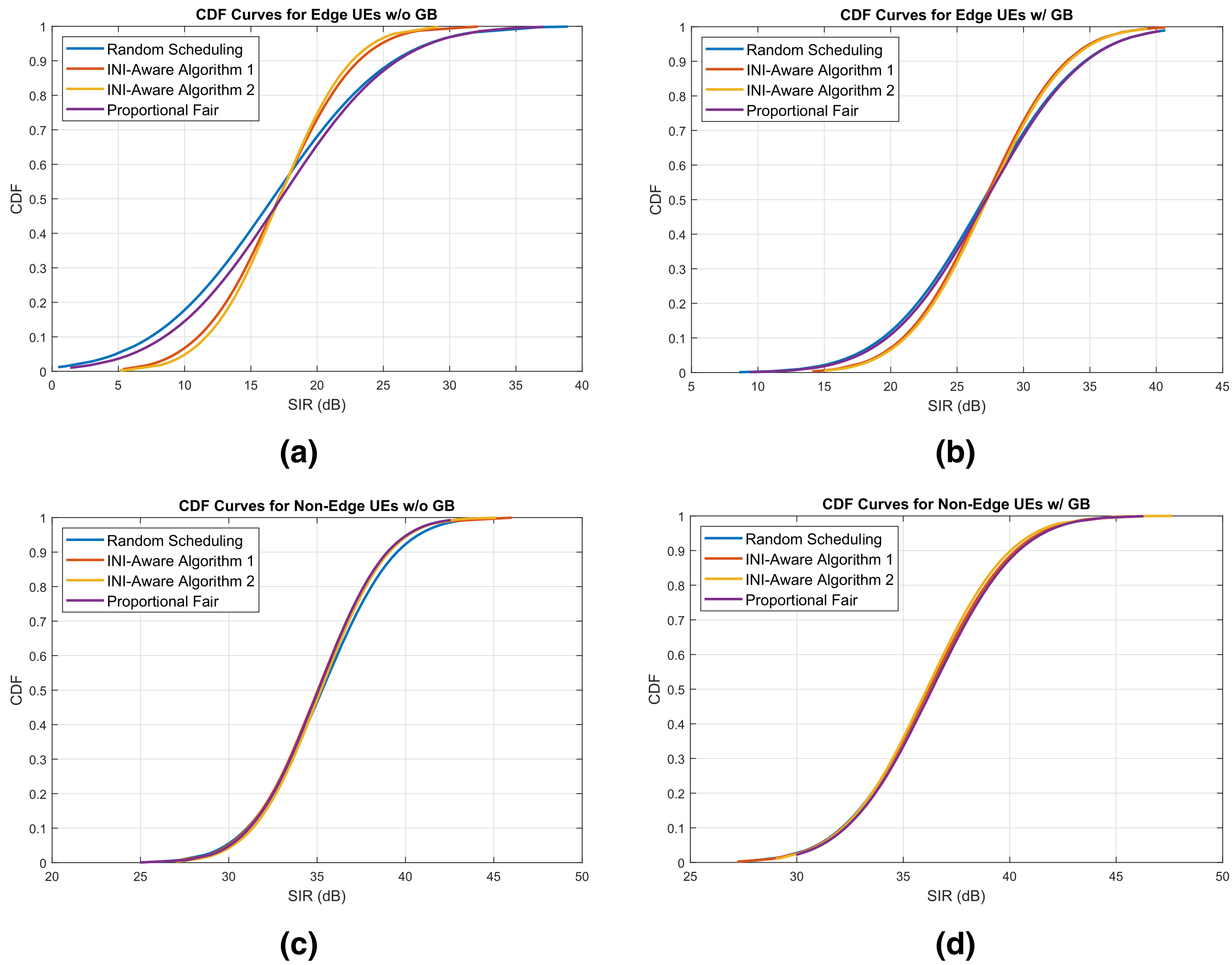

Fig. 9 The proposed fairness-aware scheduling algorithms compared to random scheduling. NUM-1 has a narrow SCs with 15 kHz Δf, and NUM-2 has a wide SCs with 30 kHz Δf. **a** CDF curves for the edge UEs without GB. **b** CDF curves for the edge UEs with GB. **c** CDF curves for the non-edge UEs without GB. **d** CDF curves for the non-edge UEs with GB

scheduling for the edge UEs. PF scheduling is not the best for the edge UEs as it is expected but it increases reliability of edge UEs slightly compared to the random scheduling. All scheduling methods give similar results for the non-edge UEs as shown in Fig. 9c, d. GB usage decreases the variation in the results of different algorithms. However, the proposed algorithms and GB usage provide the best reliability together for the numerology edges.

4 Conclusions

5G systems are designed to achieve better flexibility in an effort to support diverse services and user requirements. It is possible to apply our adaptive scheduling algorithms in multi-numerology 5G systems to enhance the reliability under the flexibility aspects of 5G NR.The proposed algorithms can be combined with user-numerology association methods and adaptive guard concepts. Meanwhile, reliability perspectives need to be handled cautiously. This type of advanced radio resource management techniques needs to be designed and optimized for multi-numerology-based NR. Implementation-dependent parts of the 5G standardization offer many other flexibility aspects that can be exploited as research opportunities.

As a future work, machine learning and deep learning techniques can be employed instead of the heuristic algorithms. Large datasets need to be constituted with practical methods for machine learning and deep learning techniques. Additionally, the proposed algorithms can be implemented for advanced waveforms like windowed OFDM and universal filtered multi-carrier (UFMC) designs as another future work.

Abbreviations

3GPP: 3rd generation partnership project; 5G: 5th generation; BS: Base station; BW: Bandwidth; BWP: Bandwidth part; CDF: Cumulative distribution function; CSI: Channel state information; eMBB: Enhanced mobile broadband; DFT: Discrete Fourier transform; FFT: Fast Fourier transform; FND: Fractional numerology domain; ICI: Inter-carrier interference; IFFT: Inverse fast Fourier transform; INI: Inter-numerology interference; IoT: Internet of Things; ISI: Inter-symbol interference; GB: Guard band; LTE: Long-term evolution; MAC: Media access control; MLB: Machine learning-based; mMTC: Massive machine-type communications; NR: New radio; NUM: Numerology; OFDM: Orthogonal frequency division multiplexing; PDB: Power difference-based; PF: Proportional fair; PHY: Physical; PL: Power level; PO: Power offset; PRB: Physical resource block; QoS: Quality of service; SC: Subcarrier; SCS: Subcarrier spacing; SIR: Signal-to-interference ratio; UE: User equipment; UFMC: Universal filtered multi-carrier; uRLLC: Ultra-reliable and low-latency communications; W-OFDM: Windowed OFDM

Acknowledgements

This paper was supported in part by the Scientific and Technological Research Council of Turkey (TUBITAK) under grant No. 215E316.

Availability of data and materials

Please contact the corresponding author at ayazar@medipol.edu.tr.

Authors' contributions

AY carried out the simulation and drafted the manuscript. HA revised the manuscript. Both authors participated in shaping the main idea, analyzed and interpreted the results, and read and approved the final manuscript.

Authors' information

Ahmet Yazar received his B.Sc. degree in Electrical Engineering from Eskisehir Osmangazi University, Eskisehir, Turkey, in 2011 and M.Sc. degree in Electrical Engineering from Bilkent University, Ankara, Turkey, in 2013. From 2011 to 2013, he was a member of the Bilkent Signal Processing Group where he studied Wavelet Theory and some other signal processing methods in various pattern recognition projects. In 2013, he joined the Information and Communication Technologies Authority and he worked in Spectrum Management Department. At the beginning of 2014, he was appointed under the Presidency of Telecommunication and Communication for 1 year. He is currently pursuing the Ph.D. degree as a member of the Communications, Signal Processing, and Networking Center (CoSiNC) at Istanbul Medipol University. His current research interests are flexible waveform systems and multi-numerology structures.

Hüseyin Arslan received his B.S. degree from the Middle East Technical University, Ankara, Turkey, in 1992, and the M.S. and Ph.D. degrees from Southern Methodist University, Dallas, TX, USA, in 1994 and 1998, respectively. From 1998 to 2002, he was with the Research Group, Ericsson Inc., NC, USA, where he was involved with several projects related to 2G and 3G wireless communication systems. Since 2002, he has been with the Electrical Engineering Department, University of South Florida, Tampa, FL, USA. He has also been the Dean of the College of Engineering and Natural Sciences, Istanbul Medipol University, since 2014. He was a part-time consultant for various companies and institutions, including Anritsu Company, Morgan Hill, CA, USA, and the Scientific and Technological Research Council of Turkey (TÜBİTAK). His research interests are in physical layer security, mmWave communications, small cells, multicarrier wireless technologies, co-existence issues on heterogeneous networks, aeronautical (high-altitude platform) communications, in vivo channel modeling, and system design.

Competing interests

The authors declare that they have no competing interests.

Publisher's Note

Springer Nature remains neutral with regard to jurisdictional claims in published maps and institutional affiliations.

Author details

[1]Department of Electrical and Electronics Engineering, Istanbul Medipol University, 34810 Istanbul, Turkey. [2]Department of Electrical Engineering, University of South Florida, Tampa, FL 33620, USA.

Received: 30 November 2018 Accepted: 18 April 2019
Published online: 02 May 2019

References

1. S. Parkvall, E. Dahlman, A. Furuskar, M. Frenne, NR: the new 5G radio access technology. IEEE Commun. Stand. Mag. **1**(4), 24–30 (2017). https://doi.org/10.1109/MCOMSTD.2017.1700042
2. A. Yazar, H. Arslan, A flexibility metric and optimization methods for mixed numerologies in 5G and beyond. IEEE Access. **6**, 3755–3764 (2018). https://doi.org/10.1109/ACCESS.2018.2795752
3. A.A. Zaidi, R. Baldemair, H. Tullberg, H. Bjorkegren, L. Sundstrom, J. Medbo, C. Kilinc, I.D. Silva, Waveform and numerology to support 5G services and requirements. IEEE Commun. Mag. **54**(11), 90–98 (2016). https://doi.org/10.1109/MCOM.2016.1600336CM
4. S. Dogan, A. Tusha, H. Arslan, OFDM with index modulation for asynchronous mMTC networks. Sensors. **18**(4) (2018). https://doi.org/10.3390/s18041280
5. L. Zhang, A. Ijaz, P. Xiao, R. Tafazolli, Multi-service system: an enabler of flexible 5G air interface. IEEE Commun. Mag. **55**(10), 152–159 (2017). https://doi.org/10.1109/MCOM.2017.1600916
6. L. Zhang, A. Ijaz, P. Xiao, R. Tafazolli, Channel equalization and interference analysis for uplink narrowband Internet of Things (NB-IoT). IEEE Commun. Lett. **21**(10), 2206–2209 (2017). https://doi.org/10.1109/LCOMM.2017.2705710
7. A. Yazar, H. Arslan, Flexible multi-numerology systems for 5G new radio. River Publishers J. Mob. Multimed. **14**(4), 367–394 (2018). https://doi.org/10.13052/jmm1550-4646.1442
8. X. Zhang, L. Zhang, P. Xiao, D. Ma, J. Wei, Y. Xin, Mixed numerologies interference analysis and inter-numerology interference cancellation for windowed OFDM systems. IEEE Trans. Veh. Technol. **67**(8), 7047–7061 (2018). https://doi.org/10.1109/TVT.2018.2826047
9. M. Richart, J. Baliosian, J. Serrat, J. Gorricho, Resource slicing in virtual wireless networks: a survey. IEEE Trans. Netw. Serv. Manag. **13**(3), 462–476 (2016). https://doi.org/10.1109/TNSM.2016.2597295
10. M. Dianati, X. Shen, K. Naik, Cooperative fair scheduling for the downlink of CDMA cellular networks. IEEE Trans. Veh. Technol. **56**(4), 1749–1760 (2007). https://doi.org/10.1109/TVT.2007.897209
11. Y. Lin, W. Yu, Fair scheduling and resource allocation for wireless cellular network with shared relays. IEEE J. Sel. Areas Commun. **30**(8), 1530–1540 (2012). https://doi.org/10.1109/JSAC.2012.120920
12. S. Mosleh, L. Liu, J. Zhang, Proportional-fair resource allocation for coordinated multi-point transmission in LTE-advanced. IEEE Trans. Wirel. Commun. **15**(8), 5355–5367 (2016). https://doi.org/10.1109/TWC.2016.2557328
13. L. Zhang, A. Ijaz, P. Xiao, A. Quddus, R. Tafazolli, Subband filtered multi-carrier systems for multi-service wireless communications. IEEE Trans. Wirel. Commun. **16**(3), 1893–1907 (2017). https://doi.org/10.1109/TWC.2017.2656904
14. 3rd Generation Partnership Project (3GPP), NR; physical channels and modulation, technical specification 38.211. ver. 15.2.0 (2018). http://www.3gpp.org/ftp//Specs/archive/38_series/38.211/
15. J. Jeon, NR wide bandwidth operations. IEEE Commun. Mag. **56**(3), 42–46 (2018). https://doi.org/10.1109/MCOM.2018.1700736
16. P. Guan, D. Wu, T. Tian, J. Zhou, X. Zhang, L. Gu, A. Benjebbour, M. Iwabuchi, Y. Kishiyama, 5G field trials: OFDM-based waveforms and mixed numerologies. IEEE J. Sel. Areas Commun. **35**(6), 1234–1243 (2017). https://doi.org/10.1109/JSAC.2017.2687718
17. A.F. Demir, H. Arslan, in *2017 IEEE 28th Annual International Symposium on Personal, Indoor, and Mobile Radio Communications (PIMRC)*. The impact of adaptive guards for 5G and beyond, (2017), pp. 1–5. https://doi.org/10.1109/PIMRC.2017.8292413
18. C. Jiang, H. Zhang, Y. Ren, Z. Han, K. Chen, L. Hanzo, Machine learning paradigms for next-generation wireless networks. IEEE Wirel. Commun. **24**(2), 98–105 (2017). https://doi.org/10.1109/MWC.2016.1500356WC
19. R. Li, et al., Intelligent 5G: when cellular networks meet artificial intelligence. IEEE Wirel. Commun. **24**(5), 175–183 (2017). https://doi.org/10.1109/MWC.2017.1600304WC
20. Q. Mao, F. Hu, Q. Hao, Deep learning for intelligent wireless networks: a comprehensive survey. IEEE Commun. Surv. Tutor. **20**(4), 2595–2621 (2018). https://doi.org/10.1109/COMST.2018.2846401